Classification and Characterization of Tropical Precipitation Based on High-Resolution Airborne Vertical Incidence Radar. Part I: Classification

BART GEERTS AND YU DAWEI

University of Wyoming, Laramie, Wyoming

(Manuscript received 6 September 2003, in final form 20 May 2004)

ABSTRACT

Airborne measurements of vertical incidence radar reflectivity and radial velocity are analyzed for some 21 231 km of high-altitude flight tracks over tropical precipitation systems, in order to describe their characteristic vertical structure. The strength of the radar dataset lies in its superb vertical resolution, sufficient to detect unambiguously a bright band and the coincident Doppler velocity change, which identify the melting layer in stratiform precipitation. In this first of a two-part study, a technique based on the detection of this stratiform precipitation signature is developed to classify hydrometer profiles as convective, stratiform, or shallow. Even though the profiles are classified individually, stratiform and convective regions emerge, whose characteristics are described. The hydrometeor vertical velocity variability is smaller in stratiform profiles, which is consistent with the physical concept of a stratiform region. The purpose of the classification is to describe, in Part II, the composite vertical structure of the various rain types in hurricanes, as well as in isolated to organized precipitating convection sampled in Florida and Brazil.

1. Introduction

The spectrum of precipitating systems at low latitudes covers a broad range of spatial and temporal scales, ranging from shallow precipitating cumuli to long-lived mesoscale convective systems (MCSs; Lopez 1976; Johnson et al. 1999). Then there are larger-scale tropical disturbances that, once developed into mature cyclones, are balanced circulation systems that are very close to symmetric neutrality (Emanuel 1986). A fundamental distinction exists between convective and stratiform precipitation within all of these systems (Houze 1997). Stratiform hydrometeors fall from the upper cloud layers while they grow (Houze 1993), and they produce a thin but distinct radar reflectivity maximum at the freezing level, known as the bright band (BB; Battan 1973). The melting of snow at the BB causes a sudden increase in fall speed (Williams et al. 1995). In convective regions a BB is absent, and the fall speed increase below the freezing level is more gradual, or absent. The rain-type distinction is important because of differences in reflectivity (Z)–rain rate (R) relationships (e.g., Steiner and Houze 1997), and different profiles of latent heating, which in turn is important in the atmosphere's general circulation (e.g., Schumacher and Houze 2003).

The convective (C)/stratiform (S) distinction between the two rain types is not new. The concept originated in the early days of radar meteorology and the separation methods have evolved. For instance, Houze (1973) used rainfall duration and intensity, inferred from tipping-bucket rain gauge data, to define ''cellular'' versus larger-scale precipitation. Subsequently, C/S separation techniques based on reflectivity maps from scanning ground-based radars were developed (Churchill and Houze 1984; Steiner et al. 1995; Biggerstaff and Listemaa 2000). These radars operate at low elevation angles, that is, essentially horizontally. Therefore, the main problem facing these C/S separation methods is the dependence of vertical resolution on range. For instance, at a representative range of 100 km, the beamwidth of the weather radars currently in operation in the United States (the Weather Surveillance Radar-1988 Doppler) is 1620 m. Such vertical resolution is inadequate to resolve the BB, which characterizes stratiform precipitation. The C/S discrimination of ground radar echoes, therefore, does not attempt to detect a BB, but examines the horizontal structure, namely, the intensity and relative isolation of echoes mapped by a low-elevation radar scan. These arguments are based on the dynamics of buoyancy-driven updrafts, which are responsible for convective precipitation. Such updrafts, compared to ascent that produces stratiform precipitation, are distinctly more intense, shorter lived, and smaller in scale (Steiner et al. 1995). Regions of convective precipitation are characterized by a fluctuating pattern of deep updrafts of at least 1 m s^{-1} (Houze 1997). Such updrafts produce rimed snow crystals, graupel, and/or hail, and, thus, no

Corresponding author address: Dr. Bart Geerts, Department of Atmospheric Sciences, University of Wyoming, Laramie, WY 82071. E-mail: geerts@uwyo.edu

BB. Thus, the classification of rain types can be based on arguments of either vertical or horizontal structure and, because the arguments are dynamically consistent, they should agree reasonably well. Practically, the choice depends on the incidence angle of the radar beam.

When a high vertical resolution is available, as is the case for profiling radars, then the C/S classification can be based at least partly on the detection of a melting-layer signature (e.g., Rosenfeld et al. 1995). The clear definition of a radar BB and of a Doppler velocity shift near the melting layer is a direct, unambiguous sign of the stratiform nature of the precipitation (Stewart et al. 1984; Houze 1993, his Fig. 6.2; Williams et al. 1995; Tokay et al. 1999). To detect and describe the BB, a high and range-independent vertical resolution is needed. In this study we use vertically incident Doppler radar data with a range resolution of less than 50 m. The precipitation radar (PR) on the Tropical Rainfall Measuring Mission (TRMM) satellite has a nearly vertical perspective, but it is also scanning within a reasonably wide swath (220 km), so its rain-type classification can be based on both vertical structure and horizontal texture arguments (Iguchi et al. 2000).

The objective of this two-part study is to classify tropical precipitation systems according to their vertical profile of reflectivity and vertical velocity, and to use this classification to describe the finescale vertical structure characteristic of precipitation systems in three regions in the Tropics. This paper (hereinafter Part I) focuses on the rain-type classification. The classification is examined, especially in terms of the characteristics and the detectability of the BB. The second part of this study (Geerts and Dawei 2004; hereinafter Part II) uses the classification results of Part I to describe typical reflectivity, vertical velocity, and upwelling microwave radiation characteristics of the various rainfall types over the ocean and over land. Both parts are based on a total of 21 231 km of the Earth Resources (ER)-2 Doppler radar (EDOP) profiles and passive microwave signatures across select tropical cyclones over the tropical Atlantic, and storms in central Florida and in the Amazon basin.

The processing and resulting accuracy of EDOP data are described in section 2. The C/S classification of rain profiles is developed and evaluated in section 3. In particular, we examine the sensitivity of the classification to vertical resolution, the properties of the melting layer, and the vertical velocity characteristics of hydrometeors in convective and stratiform regions.

2. Data sources

a. Field campaigns

This study uses the nadir-pointing 3.12-cm Doppler radar (EDOP, described in Heymsfield et al. 1996) aboard an ER-2 aircraft, which typically flies at 20 km above sea level. The EDOP range resolution is 37.5 m

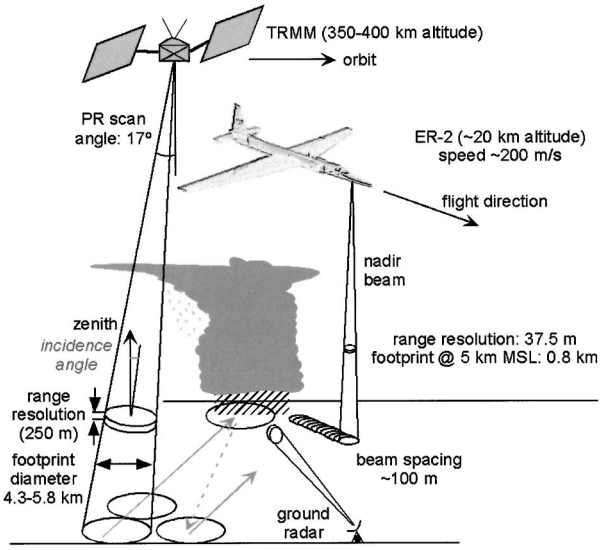

FIG. 1. Schematic of the TRMM PR and EDOP sampling strategies and resolution volumes. TRMM was raised from 350 to 402.5 km on 22 Aug 2001.

(Fig. 1), which is sufficient to detect and describe the melting-layer signature. The data were collected in three TRMM ground validation campaigns in 1998–99, namely, the third field campaign in the Convection and Moisture Experiment (CAMEX-3), the Texas and Florida Underflights (TEFLUN-B) field experiment, and the TRMM component of the Brazilian Large-Scale Biosphere–Atmosphere experiment (LBA). CAMEX-3 was aimed at Atlantic hurricanes and tropical depressions, while TEFLUN-B and TRMM-LBA focused on summertime precipitation systems over land, over central Florida, and over Rondonia in the southwestern corner of the Amazon basin, respectively. This study analyzes EDOP reflectivities and Doppler velocities from the EDOP nadir beam only. Continuous files are divided into smaller files, each corresponding to a straight and level flight track, and the data size was further reduced by focusing on precipitation features. No flight leg with good EDOP data collected in any of the three campaigns is excluded in this analysis (Table 1).

Zenith-pointing ground-based radars have been used for a long time to study the detailed vertical structure of precipitating systems (e.g., Donaldson 1961; Atlas 1966; Hobbs et al. 1985). The vertical resolution of EDOP is about an order of magnitude better than that of the lower-frequency ground-based profiling radars (e.g., Williams et al. 1995) and the X-band TRMM PR. The latter has a gate spacing of 250 m (Fig. 1), but the vertical resolution is worse for the off-nadir beams because the sampling volume is tilted (Heymsfield et al. 2000).

b. EDOP reflectivity

The EDOP profiles of the equivalent radar reflectivity factor (reflectivity, for short) and radial velocity are re-

TABLE 1. The ER-2 flights included in this study. The third column is the cumulative distance of all straight and level flight tracks along which both EDOP and AMPR data were collected, and the fourth (fifth) column lists the number of rain (surface rain) profiles according to Fig. 2.

Location	ER-2 flight dates	Total track length (km)	No. rain profiles	No. surface rain profiles	Reference name
Tropical cyclones or depressions (TD) in the Atlantic or Gulf of Mexico	23, 24, 26 Aug 1998 (Bonnie); 2 Sep 1998 (Earl); 17 Sep 1998 (TD 8); 21, 22, 25, 27 Sep 1998 (Georges)	14 437	115 542	101 647	Hurricane
Rondonia, Brazil	24, 25, 27, 30 Jan*; and 1, 5, 7, 10, 12, 17, 21, 23, 25 Feb 1999	4611	23 700	18 110	Brazil
Central Florida	8, 13, 15 Aug; and 5 Sep** 1998	2183	14 774	7201	Florida

* AMPR data are not available for 25 Jan 1999, but EDOP data are used for this day, over a distance of 977 km.
** Only during 2217–2238 UTC; the earlier part of the flight samples a precipitation region offshore from Cape Canaveral, Florida.

corded every 0.5 s, which corresponds with an along-track distance of roughly 100 m. The radial velocity field, as well as the derived vertical airflow, are thresholded by the requirement that the reflectivity exceeds 0 dB*Z*. This value is a few dB*Z* above the EDOP sensitivity threshold at a range of 20 km for all campaigns in this study, and is 18 dB*Z* more sensitive than the TRMM PR. The threshold ensures that no noise is included in the radial velocity statistics.

The rain-type classification, discussed in section 3, depends on EDOP reflectivity values and, therefore, EDOP calibration and signal attenuation rates need to be considered. The accuracy of the EDOP nadir reflectivity values has been confirmed by means of a comparison with coincident TRMM PR and ground radar data (Heymsfield et al. 2000). At 9.6 GHz, a 5-km-deep layer of rain with a reflectivity of 39 dB*Z* results in a two-way path-integrated attenuation of merely 1 dB*Z*. Therefore, attenuation is insignificant for most of the profiles analyzed here. In the case of vigorous convection, as observed over Florida, attenuation may be important (Tian et al. 2002), but when using one wavelength and one beam it is difficult to estimate, in part because of its sensitivity to the hydrometeor types in the profile, and in part because of the variability of the surface cross section of the underlying land surface. Thus, the EDOP reflectivities have not been corrected for attenuation. In any event, the profiles with the highest reflectivities are unambiguously classified as convective, irrespective of attenuation correction.

c. EDOP nadir radial velocity

The radial velocities have been corrected for aircraft motion using the method of Lee et al. (1994), which is based on Heymsfield (1989). The correction has some uncertainties, mainly those related to aircraft position (based on both differential GPS and the Inertial Navigation System) and the position of the antenna in the nose of the ER-2 aircraft. The standard deviation of the radial velocity at the earth's surface, where the radar reflectivity spikes, averages at 1.57 m s^{-1} in the three regions. This variability may be due to errors in the correction for aircraft motion, but nonlevel terrain, especially in Brazil, and wind-driven capillary waves, near hurricanes, can produce a nonzero radial velocity at the surface when the antenna is slightly off nadir. Mean radial velocities at the earth's surface were found, respectively, to be -0.66, -1.40, and -0.96 m s^{-1} for the Florida, hurricane, and Brazil samples listed in Table 1. Negative values imply that the ground tends to rise. These systematic biases are most likely due to a forward tilt of the nadir antenna. (A mere 0.25° antenna offset implies a 1 m s^{-1} bias for a 200 m s^{-1} aircraft speed.) Testud et al. (1995) derived a variational method to reduce airborne Doppler velocity errors by analyzing the returns of a flat earth surface as a function of the antenna rotation angle. This method does not apply to straight flight legs, because the range of nadir angles is too small. We merely adopted a simple improvement: the radial velocities in the three regions were corrected by the respective average biases at the earth's surface. The remaining radial velocity uncertainty should be 1 m s^{-1} or less (Heymsfield and Tian 2000; G. M. Heymsfield 2001, personal communication), and is likely highest in the hurricane sample, because of contamination by horizontal winds when the beam is off nadir. The latter cannot be corrected for because the horizontal winds below the flight track are not known. The resulting errors tend to cancel in a composite sense because storms were usually transected many times, from opposite directions. This reduces the mean error but not its variability. This uncertainty should be kept in mind when interpreting composite velocity results shown later.

d. Vertical air motion

The vertical air motion is derived from the corrected nadir beam radial velocity, assuming height-dependent relationships between hydrometeor terminal velocity V_p and radar reflectivity factor Z for rain, snow, and graupel (see the appendix). Clearly, the estimated fall speed is uncertain, especially in convective precipitation and near the BB. Its uncertainty is comparable in magnitude to the uncertainty in radar radial velocities (section 2c).

Therefore, the derived instantaneous vertical air motion has an uncertainty on the order of 2 m s^{-1} (i.e., $\sqrt{1} + \sqrt{1}$) because it is affected by uncertainties both in hydrometeor motion and in terminal velocity estimation. The uncertainty of the mean vertical air motion is smaller. In vigorous convection both terms may be 2 times as large, resulting in an air motion uncertainty of 3 m s^{-1}.

3. Rain-type classification

There is no unique way to separate convective from stratiform precipitation. Any method has to be tailored to radar's vantage point. In the case of ordinary ground-based scanning radars, the scans have the best resolution and continuity in the horizontal plane, and so horizontal texture methods (e.g., Churchill and Houze 1984; Steiner et al. 1995) are the most appropriate.

The EDOP radar, on the other hand, provides a rich vertical description but little horizontal context. The reason is that EDOP is a fixed antenna device, that is, it does not scan in a direction normal to the flight track. The aircraft motion adds an along-track dimension, so EDOP essentially provides vertical cross sections. These sections are similar to those obtained from profiling ground-based radars (e.g., Gage et al. 2002), except that the latter combine evolution and translation whereas EDOP transects are quasi instantaneous. In comparison with the TRMM PR, which does provide a horizontal context, EDOP has both a better vertical resolution and Doppler information. Thus, the EDOP-based classification is based on profiles of reflectivity and velocity.

As discussed in Houze (1997), the rain-type separation should be based on the physical concept of stratiform and convective *regions*: a convective region should contain active deep convection (i.e., the overturning of air on a small scale). A stratiform region in the Tropics contains decaying convection, with weaker vertical velocities and fewer, weaker local updrafts. Stratiform regions in tropical cyclones are fundamentally different; they can be sustained by the storm-scale circulation (e.g., Marks et al. 1992).

Because the EDOP-based classification method uses vertical information only, each reflectivity profile must be classified individually. This implies that an individual storm can have closely spaced rain types in a transect, for example, convection can be embedded in stratiform precipitation. The only size constraint is that rain-type regions are only retained if at least five consecutive profiles have the same classification. This corresponds to a minimum width of ~500 m, which is comparable to EDOP's beamwidth (Fig. 1). The four or fewer isolated profiles are ignored, unless they are surrounded by profiles of the same rain type (e.g., stratiform), in which case they are assumed into the region of that rain type. Such a measure eliminates borderline cases that jump between one type and another. However, because of EDOP's oversampling, this criterion turns out to have little or no impact on the continuity of rain types. Thus, this minimum size threshold is insignificant in comparison with the real spatial continuity of rain types in EDOP profiles (to be discussed later). The more continuous regions of stratiform precipitation will more closely correspond to the physical concept of a stratiform region as clarified by Houze (1997).

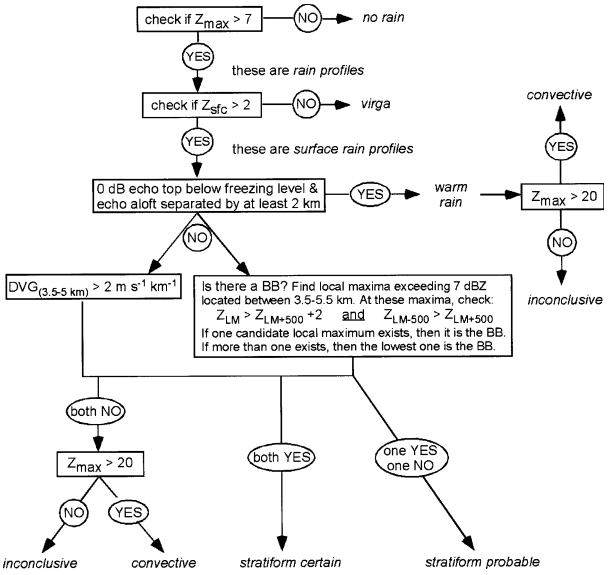

FIG. 2. Flowchart for the classification of EDOP nadir reflectivity beams: Z refers to the filtered equivalent reflectivity (dB), Z_{lm} is its value at a local maximum (lm), Z_{max} is its profile maximum value, Z_{sfc} is the minimum reflectivity just above the strong echo from the earth surface, and $DVG_{(3.5–5km)}$ is the Doppler velocity gradient between the heights of 3.5 and 5 km.

a. Definition

EDOP reflectivity and velocity profiles represent a unique opportunity to characterize the vertical structure of convective and stratiform precipitation, because of the high vertical resolution and the clutter-free nature down to ground level. Precipitation types in essence are discriminated based on the presence of a melting-layer signature, which characterizes deep stratiform precipitation. This signature includes a BB and a rapid increase in hydrometeor fall speed, which is evident as a large Doppler velocity gradient (DVG; Houze 1993, his Fig. 6.2).

Only profiles with an equivalent reflectivity of at least 7 dBZ at some level are considered, and they are referred to as ''rain profiles'' (Table 1). First, the near-surface reflectivity minimum is evaluated. If it less than 2 dBZ, then rain does not reach the ground (referred to as *virga*) (Fig. 2). Of all rain profiles in the dataset, 17% contain only virga. The remainder is referred to as ''surface rain profiles.'' Clearly, the category of EDOP-based virga profiles is quite different from the population of virga inferred from TRMM PR profiles.

Local reflectivity maxima close to the freezing level, that is, between a 3.5- and 5.5-km altitude, are identified next. These maxima are considered candidate BBs if (a) the reflectivity 500 m below (Z_b) exceeds the reflectivity 500 m above (Z_a), and (b) the local maximum reflectivity (Z_{lm}) exceeds Z_a by at least 2 dB*Z*. If this process yields more than one candidate, the lowest one is selected to be the BB. If a BB is present then this beam is likely to be stratiform. This is broadly consistent with the 2A23 TRMM PR algorithm *V* method of rain-type classification (NASDA 1999).

Another melting-layer characteristic is a large DVG across the melting layer, resulting from a change from snow to rain. All proximity soundings for the flights listed in Table 1 had a freezing level between 4.4 and 4.9 km. A steady stratiform precipitation produces a ~200 m deep isothermal layer at 0°C, the BB peaks some 300 m below that, and melting snow should be all rain some 300 m below the BB peak (Stewart et al. 1984). Therefore, the entire change of fall speed should be contained between 3.5 and 5 km. Williams et al. (1995) and Tokay et al. (1999) use a DVG value of 2 m s^{-1} km^{-1} in this layer as a threshold for stratiform precipitation in the Tropics. The same value is used here. It should be noted that the DVG is not affected by the uncertainty in hydrometeor vertical velocity due to aircraft motion (section 2c); any error is constant with range, that is, height independent.

If both a BB is present and the DVG between 3.5 and 5 km exceeds 2 m s^{-1} km^{-1}, then the profile is considered to be certainly stratiform. If only one condition applies, then the profile is probably stratiform (Fig. 2).

If neither condition applies, and the maximum reflectivity is larger than 20 dB*Z*, then this beam is classified as convective. For the other cases, the beam's rain type is classified as inconclusive in analogy with the TRMM PR *V*-method rain-type classification. However, the threshold value used here for inconclusive precipitation is much lower than that of TRMM (39 dB*Z*) (NASDA 1999), because most inconclusive profiles with peak reflectivities between 20 and 39 dB*Z* clearly appear convective in echo and vertical velocity structure. In contrast to TRMM, our inconclusive profiles are rather insignificant in terms of their contribution to surface rainfall.

The rain-type classification is illustrated for a small MCS in Brazil in Fig. 3. A broad area of anvil precipitation can be seen on the left, with some mammatalike protuberances at the base of the anvil. Convective and stratiform regions are relatively coherent. The stratiform precipitation regions have a clearly visible BB (top panel) and DVG (middle panel). Inconclusive profiles are interspersed with convective ones, depending on whether the maximum reflectivity exceeds 20 dB*Z*.

b. Along-track C/S fraction and rain-type regions

We now provide some simple statistics of the rain-type classification. Such statistics not only assess the classification but also reveal differences between storms sampled in the three regions. According to the EDOP-based classification method, 19%–36% of all surface rain profiles is convective, while 34%–67% is probably or certainly stratiform (Table 2). It should be mentioned that the C/S fractions mentioned here and elsewhere in the paper refer to the number of profiles. The rainfall amounts, such as the convective rain fraction, are not estimated, because it is sensitive to the reflectivity–rain rate relationship selected. The along-track convective fraction used here is the one-dimensional equivalent of the convective (rain) area fraction, which has been estimated in many studies (e.g., Churchill and Houze 1984; Steiner et al. 1995; Schumacher and Houze 2003).

A fundamental distinction exists between the ''hurricane'' sample, which is mainly stratiform, and the precipitation systems in Florida and Brazil. However, even in the latter two regions the stratiform fraction is relatively high, about as high as the convective fraction. This is consistent with the relative ubiquity of stratiform precipitation in the Tropics (Houze 1997), even over land. The stratiform fraction in central Florida is the highest, and is significantly higher than in Brazil (Table 2), which is consistent with Petersen and Rutledge (2001). In Brazil, nearly one-half of the profiles have no melting-layer signature and are too weak to be called convective (i.e., inconclusive).

Schumacher and Houze (2003) show that the stratiform rain area fraction is 73% in the Tropics (20°N–20°S), according to 3 yr of TRMM PR data (2A23 algorithm). In that study the stratiform group includes the inconclusive and intermediary classes. Thus, the comparison is more correct if we look at the convective rain area fraction, which then averages 27% in the Tropics. In the southwestern Amazon (the state of Rondonia), the study finds the convective rain area fraction to be about 21% in the southern summer (December–February; C. Schumacher 2004, personal communication), slightly less than the average for the 1D EDOP sample (24%, Table 2). The EDOP observations were taken in late January and February, that is, in the second half of the rainy season, when the convective area fraction is believed to be lower (Petersen et al. 2002). Central Florida is not included in the Schumacher and Houze (2003) analysis, but the precipitation there probably behaves similarly to that over other small landmasses surrounded by warm water, such as the Top End region in northern Australia in the southern summer. The Schumacher and Houze study finds a convective area fraction of about 25% there, certainly lower than in the Amazon, but less than the average for the EDOP Florida sample (36%). At least the higher along-track convective area fraction in Florida (as compared with Brazil) in our study is consistent with the higher convective area fraction of the Top End in comparison with that of Rondonia in the Schumacher and Houze study.

When we degrade the EDOP resolution to 250 m (that of the TRMM PR at nadir), then the convective area

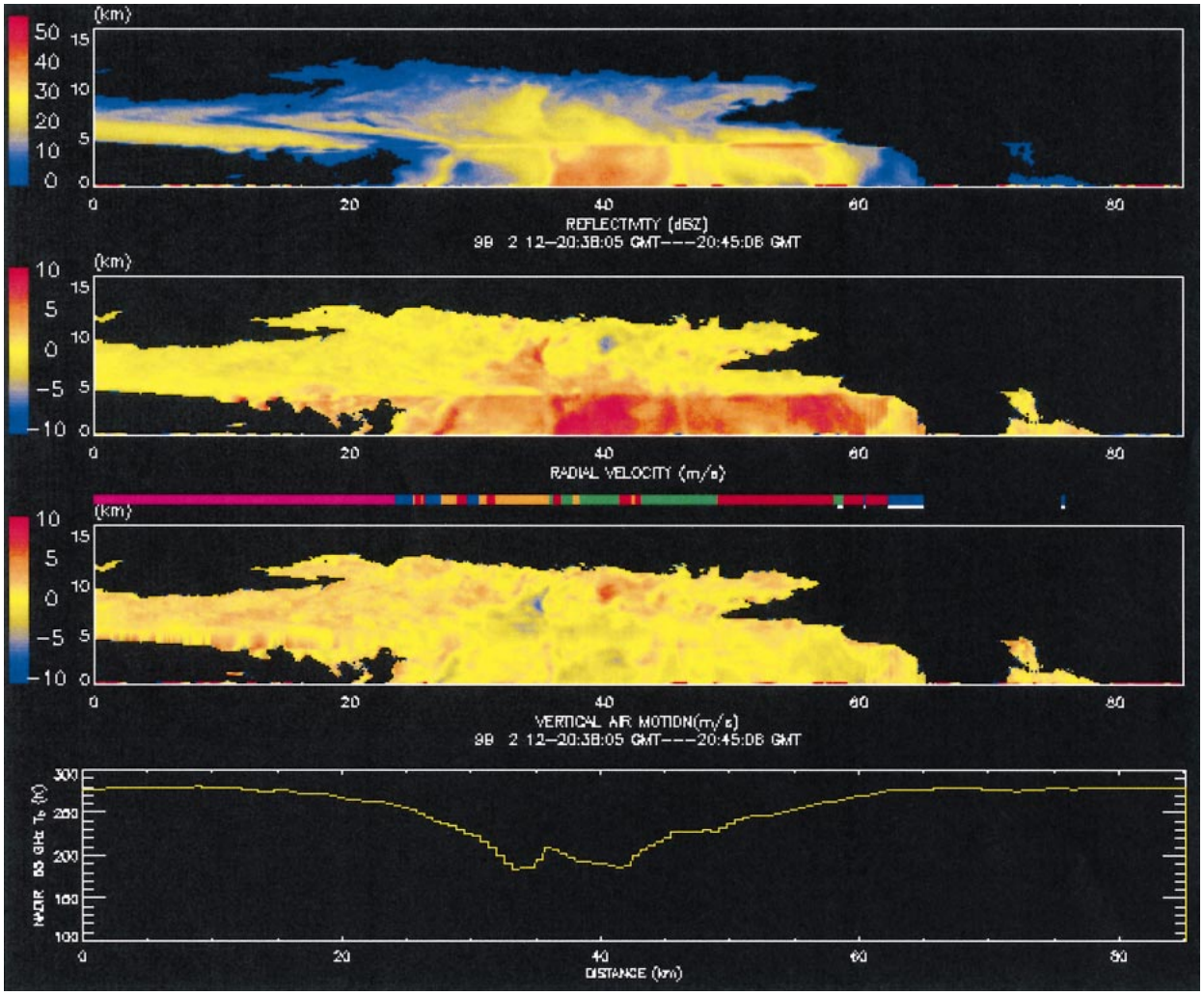

FIG. 3. A sample cross section across a small MCS in Brazil, between 2038 and 2045 UTC 12 Feb 1999. The vertical axis for the first three images is height above sea level (km), as detected by EDOP. Displayed are the (a) EDOP nadir reflectivity (dBZ), (b) radar radial velocity corrected for aircraft motion (this is the hydrometeor vertical velocity, m s^{-1}, where downward is positive), (c) air vertical velocity (m s^{-1}), and (d) coincident microwave brightness temperature at 85 GHz, measured by the Advanced Microwave Precipitation Radiometer (AMPR). The rain-type classification bar shown between (b) and (c): certainly stratiform, (red), probably stratiform (orange), convective (green), inconclusive rain (blue), virga (purple), and no rain (black).

fraction increases by about 14% in all regions, because of a lower detectability of the melting-layer signature (Table 2). Also, the elimination of all profiles weaker than 18 dBZ just above the surface (the sensitivity of the TRMM PR) further increases the convective area fraction by 2% on average in all regions. Thus, the EDOP data suggest a higher convective area fraction than the TRMM PR climatology indicates. This may be due to selective sampling of EDOP data (flight tracks were generally designed to cover larger, more intense, more persistent storms), and/or a tendency for our algorithm to yield a higher convective fraction than the TRMM PR 2A23 algorithm. The vertical structure of hurricanes and precipitation systems in Florida and Brazil will be explored further in Part II.

Even though profiles are classified individually, and there is no proximity argument for the horizontal rain-type classification (e.g., Steiner et al. 1995), profiles of a certain rain type occur grouped in regions (Table 2). We can only determine the along-track length of these regions, not their area. The lengths listed in Table 2 are limited, of course, by the total length of the straight and level flight tracks, but these tracks generally cover entire precipitation features. Stratiform regions tend to be larger than convective regions, and those in hurricanes are almost an order of magnitude larger than those in Brazil and Florida. The continuity of stratiform regions in hurricanes is obvious, for example, in EDOP transects across Hurricane Georges (Geerts et al. 2000, their Figs. 7 and 8), as well as from other studies (e.g., Marks and Houze 1987). This will be discussed further in Part II.

The average size of convective regions sampled by

TABLE 2. Along-track C/S fractions, and typical sizes of regions of various rain types, in the three tropical environments sampled by EDOP. Total number of surface rain profiles is for the above four rows, and is listed also in Table 1. In the following rows the inconclusive profiles are ignored, i.e., the sum of convective and stratiform percentages is 100%, and all stratiform profiles are counted, i.e., ''stratiform all'' refers to stratiform certain and probable. These percentages are shown for the original EDOP range resolution ($\Delta z = 37.5$ m) and a degraded resolution ($\Delta z = 250$ m). In the last six rows, the mean and maximum continuous along-track lengths of rain-type regions are shown.

Parameter	Type	Hurricane	Brazil	Florida
Fractions	Convective	19%	24%	36%
($\Delta z = 37.5$ m)	Stratiform certain	56%	16%	17%
	Stratiform probable	11%	18%	19%
	Inconclusive	14%	42%	28%
	Total No. of profiles	101 647	18 110	7201
Fractions	Convective	23%	48%	55%
($\Delta z = 37.5$ m)	Stratiform (all)	77%	52%	45%
Fractions	Convective	36%	63%	68%
($\Delta z = 250$ m)	Stratiform (all)	64%	39%	32%
Mean along-track	Convective	4.0	2.2	2.9
dimension (km)	Stratiform (all)	23.2	4.3	3.5
	Inconclusive	2.2	2.4	1.6
Max along-track	Convective	11.2	12.6	20.4
dimension (km)	Stratiform (all)	113.2	19.7	15.6
	Inconclusive	6.4	7.8	5.3

EDOP is about 2 km in Florida and Brazil. It is not clear how representative this is, because of the selective sampling of EDOP data. It is consistent with Goldhirsh and Musiani (1986), who use ground-based radar to show that the median size of convective cells in summer near the Mid-Atlantic coast of the United States is 1.9 km. Sauvageot et al. (1999) found that radar-derived rain cell size distributions from various tropical regions are roughly exponential, with a slope of 0.3–0.8 km^{-1}, and a median size of about 2 km. In tropical cyclones, convective cells appear to be larger, and the variability of cell sizes smaller (Table 3).

c. Melting-layer signature

We now examine the stratiform profiles in more detail, with a focus on the melting-layer signature. Most profiles with a BB also have a rather high DVG: the percentage of BB profiles with a 3.5–5 km DVG exceeding 2 m s^{-1} km^{-1} (stratiform certain, Fig. 2) is 92%, 71%, and 67%, respectively, for the hurricane, Brazil, and Florida samples. This indicates that the hurricane stratiform rain profiles are more clearly stratiform. Further evidence for this arises when we degrade the EDOP range resolution. To do that, we filter the reflectivity profiles by means of a running average [calculated in units of mm^6 m^{-3} (Z) before converting to dBZ units]. For instance, to represent a 250-m resolution (the TRMM PR vertical resolution at nadir), a 7-point running mean is used ($250/37.5 \sim 7$). Then the same BB detection algorithm is used as for the original EDOP data (Fig. 2). The BB becomes less detectable at coarser resolutions, especially between 250 and 1000 m (Fig. 4). (For a resolution of 1000 m, reflectivity values are

TABLE 3. A comparison between two criteria that characterize the melting layer in stratiform precipitation. These are (a) whether a BB is present, as defined in section 3a (BB yes/no), and (b) whether the DVG exceeds 2 m s^{-1} km^{-1} in the layer between 3.5 and 5 km (DVG yes/no). All surface rain profiles listed in Table 1 are used (except, of course the warm rain profiles), but the numbers are shown as percentages. The p value between parentheses is the probability that if the DVG and BB criteria are mutually independent a random sample exceeds the χ^2 value of this comparison, for each region.

	DVG yes	DVG no
Hurricane ($p = 10^{-12}$)		
BB yes	60.4	5.0
BB no	6.9	27.6
Brazil ($p = 10^{-6}$)		
BB yes	17.0	7.1
BB no	12.8	63.2
Florida ($p = 10^{-5}$)		
BB yes	18.0	7.7
BB no	12.5	61.8

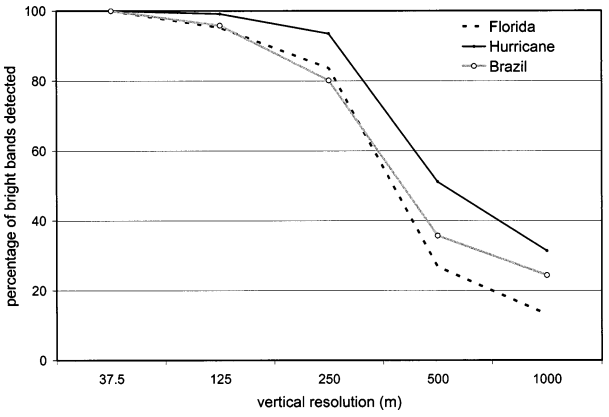

FIG. 4. The BB detection rate as a function of vertical resolution. The number of profiles with a BB is expressed as a percentage of the ''true'' total, i.e., those detected at EDOP resolution. The vertical resolution is reduced by smoothing the EDOP profiles.

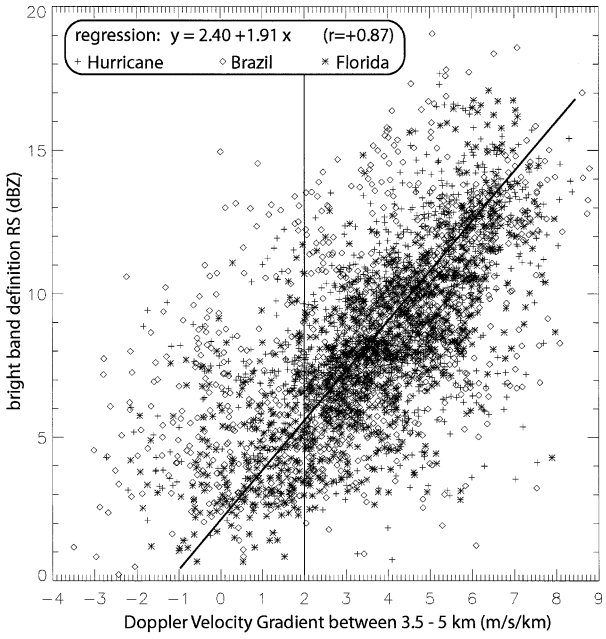

FIG. 5. Scatterplot of DVG (m s^{-1} km^{-1}) between 3.5 and 5 km vs the reflectivity spikiness RS (dB*Z*) for all profiles with a BB. The slant line is the regression best-fit line.

linearly interpolated with height to evaluate the BB criterion.) Thus, a degraded resolution implies a lower stratiform area fraction (Table 2). This loss in BB detectability is remarkably larger in the Brazil and Florida samples than in the hurricane sample (Fig. 4). As a result, the hurricane stratiform area fraction stands out increasingly above that of the two other regions when the resolution is degraded. Thus, the stratiform profiles are more clearly stratiform in the hurricane sample.

The high resolution of the EDOP profiles allows an estimation of the sharpness or strength of the BB. We compute an index we call the ''reflectivity spikiness'' (RS),

$$\mathrm{RS} = Z_{\mathrm{bb}} - (Z_a + Z_b)/2,$$

where Z_{bb} is the reflectivity at the BB, and Z_a (Z_b) is the reflectivity at 500 m above (below) the BB. All reflectivity values are expressed in dB*Z*. A scatterplot of RS versus DVG is shown in Fig. 5, for all stratiform profiles in three regions. A ''brighter'' BB tends to imply a stronger DVG, which has been observed elsewhere (White et al. 2002). The relation is strongest in the hurricane sample, but in all regions there is a lot of scatter. Some of this may be due to coincident changes in vertical air motion across the BB, but more important the scatter indicates that there is a range of stratiform precipitation characteristics, and that the transition from a stratiform to convective signature is ill defined. The DVG also varies with stratiform precipitation rate: the fall speed of unrimed ice crystals is relatively size independent, whereas raindrop fall speeds have a much stronger dependency on diameter (appendix). Stratiform profiles with a low mean reflectivity value (i.e., a small median diameter of snowflakes or raindrops), thus, tend to have a smaller DVG across the BB than those with high reflectivities. Especially in Brazil and Florida, many BB signatures do not have a DVG exceeding 2 m s^{-1} km^{-1}. Thus, while the DVG is a useful indicator of the melting of snowflakes and the stratiform nature of the precipitation, its magnitude does not quantify this nature.

To further examine the relation between the two aspects of the stratiform melting-layer signature, we tested all the surface rain profiles, except, of course, the warm-rain profiles (Fig. 2), for two criteria: (a) whether a BB is present (defined in section 3a), and (b) whether the 3.5–5-km DVG exceeds 2 m s^{-1} km^{-1} (Table 3). Most profiles do satisfy or dissatisfy both criteria, and the criteria disagree for few profiles. For all three regions, the χ^2 value for this analysis of variance implies that the odds are less than 0.1% that the two criteria are independent. However, the agreement between the two criteria is better for the hurricane sample, where just 12% of the surface rain profiles disagree on the two criteria, than for storms sampled over Brazil or Florida, where 20% of the profiles disagree. This again is evidence that hurricane stratiform rain is more evidently stratiform: the bulk of the hurricane profiles is ''certainly stratiform'' (Table 2). On the other hand, more profiles are classified as ''probably stratiform'' than as certainly stratiform in both Brazil and Florida.

The certainly stratiform sample has a clear melting-layer signature, but variability exists even within this sample. This is illustrated by means of a frequency-by-altitude display (FAD) centered on the BB (Fig. 6). This display shows the probability density function stratified by height, and normalized by the total number of occurrences at all levels. At each level (37.5-m increments), occurrences are binned at 1-dB*Z* intervals. The height is expressed relative to that of the maximum reflectivity in the BB, in order to better depict the composite structure of the BB. If the absolute height was used, then variations in the height of the freezing level, for instance, from the eyewall to the eye of a hurricane, would yield a blurred composite profile. It should be cautioned that the number of stratiform profiles over land is an order of magnitude smaller than that in hurricanes (Table 2). The reflectivity decay in the first few hundred meters above the BB is very similar in the three regions, about 3.5–4 dB*Z* (100 m)$^{-1}$. A clear difference between the regions can be seen about 300 m above the BB. There reflectivity continues to clearly decay in hurricanes. In stratiform profiles in Brazil and especially in Florida, the decay is much slower; and at 2 km above the BB, the average reflectivity is only 13 dB*Z* below the BB value in Florida, compared to 22 dB*Z* in the hurricane sample. In other words, the difference between land-based and hurricane stratiform precipitation is most evident well above the BB. There is also a slight tendency for hurricane reflectivity values to increase

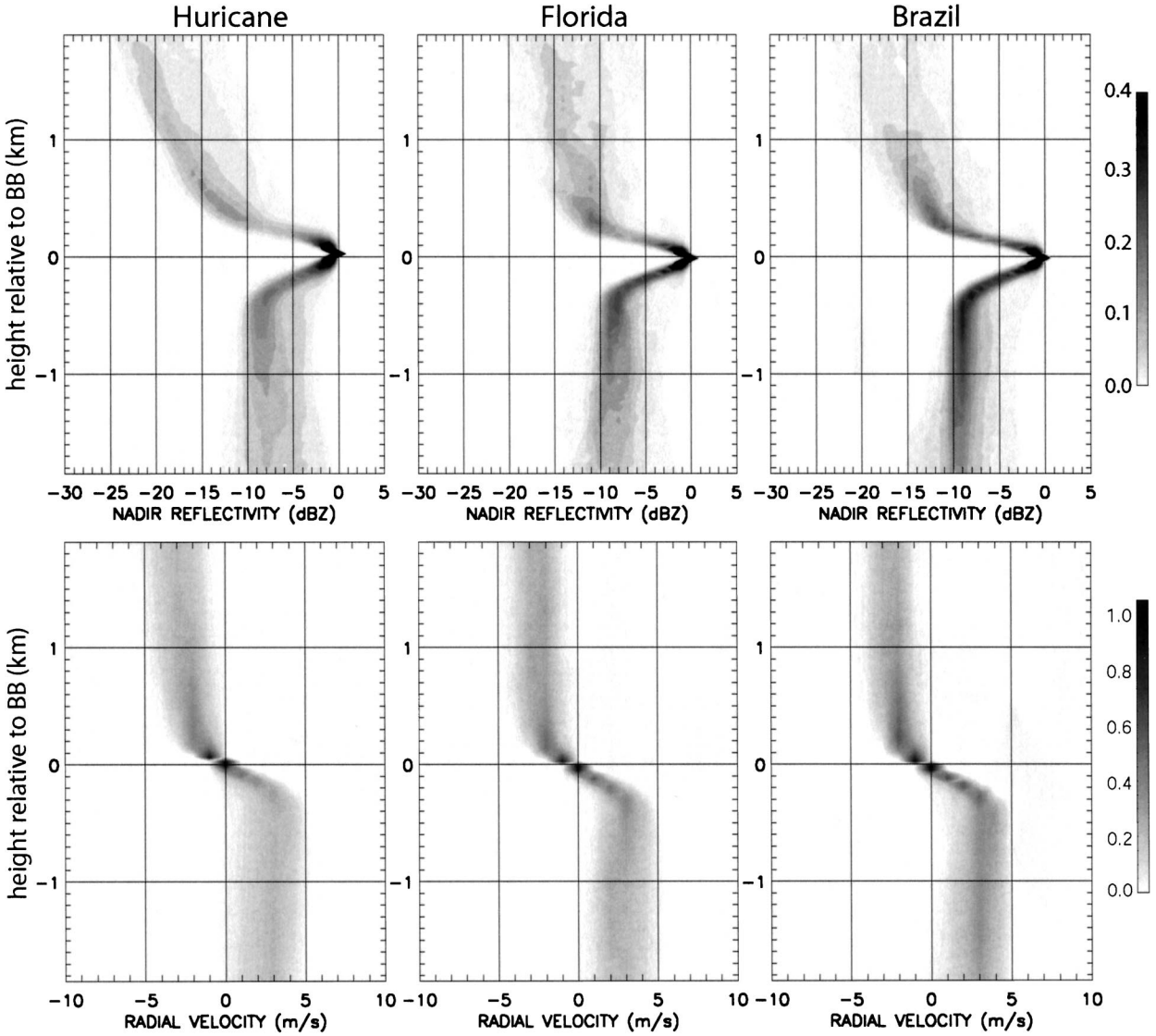

FIG. 6. Frequency-by-altitude displays of EDOP nadir reflectivity and radial velocity around the BB, for all stratiform-certain profiles in three regions. The three top panels show the reflectivity relative to the maximum value at the BB. The units are $(3\ \mathrm{dB}Z)^{-1}\ \mathrm{km}^{-1}$. The three bottom panels show the radial velocity relative to the value at the BB height $[(\mathrm{m\ s}^{-1})^{-1}\ \mathrm{km}^{-1}]$.

toward the ground, below the reflectivity minimum just below the BB. This tendency, which is not apparent in the Brazil or Florida profiles, suggests continued hydrometeor growth. The Florida profile is also more variable. Some stratiform profiles in Brazil and more in Florida have a weak BB, exceeding the ambient reflectivity (±500 m) only by a few decibels (Fig. 5).

Radial velocity composites around the BB are also shown in Fig. 6. The height of the radial velocity profile is again relative to that of the BB, and the radial velocity value is relative to that at the BB. The latter eliminates the uncertainty due to errors in the correction for aircraft motion (section 2c) and it allows focusing on the DVG. The frequency-by-altitude bin size is 1 m s^{-1}, and so some discontinuities are apparent near the BB.

All profiles are remarkably homogeneous, with a clear jump of about 5 m s^{-1} over a depth of 500 m centered near the BB. This applies not only to the hurricane sample, but also to stratiform regions in Brazil and Florida, which is consistent with the relative homogeneity in the reflectivity profiles around the BB in all regions (Fig. 6). Again, it needs to be emphasized that a large range of reflectivities and velocities exist; it is only relative to the reflectivity and velocity values at the BB that the profiles display little variability. This homogeneity suggests that the scatter due to changes in vertical air motion is small, and that the observed range of reflectivity values yields a relatively narrow range of DVG values.

In summary, a range of stratiform reflectivity and

TABLE 4. Echo vertical motion characteristics of convective, stratiform, and inconclusive surface rain profiles. Sample sizes, shown between brackets, are given as percentages in Table 2; σ_{5-10} is the standard deviation of hydrometeor vertical motion at heights between 5 and 10 km. The numbers of profiles with hydrometeor vertical velocity V_r larger than 2 m s^{-1} in magnitude is shown in the next column, again at heights between 5 and 10 km. Profiles are counted under ''lifting below 4 km'' if the hydrometeors ascend at some level below 4 km. ''Rapid lifting'' occurs if their maximum ascent rate in the profile exceeds 4 m s^{-1}. Shown are the percentages of the surface rain profiles that satisfy the given criteria.

Echo vertical motion		σ_{5-10} (m s^{-1})	$\lvert V_r\rvert_{5-10} >$ 2 m s^{-1} (%)	Lifting below 4 km (%)	Rapid lifting (%)
Hurricanes	Convective (20 329)	2.0	66	3	1.2
	Stratiform certain (57 939)	1.2	29	0.2	0.2
Brazil	Convective (4709)	3.9	82	6	3
	Stratiform certain (2898)	1.6	40	0.4	0.6
Florida	Convective (2736)	4.8	97	12	6
	Stratiform certain (1348)	2.4	51	0.5	0.4

Doppler velocity profiles exists. Not only do stratiform profiles dominate in the hurricane sample, but they are also more clearly stratiform there than in Brazil and especially in Florida. This is apparent from the good agreement between the BB and DVG aspects of the melting-layer signature, and the detectability of the BB even under poor vertical resolutions. This is a reflection of the fundamentally different circulation and life cycle of tropical cyclones, in comparison with that of isolated to organized convective systems, as sampled in Florida and Brazil.

d. Rain type and hydrometeor vertical velocity

Tropical rain profiles have been classified through a direct detection of the melting-layer signature of stratiform precipitation, that is, a BB and a large DVG. The question now arises as to whether the vertical velocity characteristics of C/S precipitation apply to the EDOP-classified rain profiles. As mentioned in the introduction, stratiform regions containing the remnants of previously active convection, are unlikely to harbor strong, small-scale updrafts; the vertical air motion is generally less than 1–2 m s^{-1} (Houze 1997, his Fig. 1). Regions of vigorous convection are characterized by a fluctuating pattern of deep updrafts of at least 1 m s^{-1}. This leads to the growth of snow crystals by riming, and graupel melts over a deeper layer than unrimed snow, resulting in a weaker DVG and a lack of BB. On the other hand, stratiform hydrometeors grow from the upper cloud layers, mainly by diffusion and aggregation. In some cases the stratiform region is clearly separated from active convection. Usually, as for the small MCS shown in Fig. 3, convection is embedded in a stratiform region, and the distinction between stratiform and convective regions is less apparent in the vertical velocity field than in the reflectivity field. The variability of vertical motions is larger in the convective region of Fig. 3. Note, for instance, a strong upper-level updraft near $x = 40$ km in the third panel of Fig. 3.

While the above argument is based on microphysical processes resulting from air vertical motion, it can be assessed more conveniently by means of hydrometeor vertical motion, that is, the Doppler radial velocity at nadir (section 2c). The latter does not carry the uncertainty of the hydrometeor terminal velocity (section 2d). In vigorous convection, hydrometeor trajectories are like fountains, with upward and downward limbs (Houze 1997, his Fig. 1). Note, for instance, the upper-level echo ascent near $x = 40$ km in the second panel of Fig. 3. In old convection, on the other hand, the trajectories are mainly downward, resulting in stratiform regions.

It should be noted that this argument applies to convective systems only, not to tropical cyclones. Updrafts in tropical cyclones, especially in the eyewall, are broader and more sustained than those in buoyancy-driven convective cells. Updrafts in the eyewall may generate both large graupel that falls at about the same radius from the eye, and smaller ice particles that are lifted into the upper troposphere without much riming, leading to stratiform precipitation at a larger radius (Houze et al. 1992). Tropical cyclones may contain vigorously convective cells as well (e.g., Geerts et al. 2000; Heymsfield et al. 2001).

We find that in most profiles hydrometeors are carried upward at some level, even in the majority of stratiform profiles, and that in terms of the mean vertical motion of the hydrometeors, the difference between convective and stratiform regions is very small, which is consistent with the findings of Williams et al. (1995, their Fig. 6). The real difference between stratiform and convective precipitation lies in the spread of vertical motion around the mean. To quantify the variability of the hydrometeor vertical motion V_r, and the examine the occurrence of hydrometeor fountains, we summarize some parameters in Table 4. The variability is evaluated above the freezing level, where V_r is not affected by the particle acceleration due to melting, and where the difference between vigorous and old convection should be most obvious. In addition, in order to assess the presence of hydrometeor fountains driven by strong ascents, we look for the existence of rapid lifting (hydrometeors are lifted at over 4 m s^{-1}) and/or shallow lifting (hydrometeors

are carried upward below the freezing level). The criteria are somewhat arbitrary, but they reflect the physical basis of the convective/stratiform separation. For simplicity, the stratiform probable and inconclusive profiles are not included in Table 4.

The contrast between convective and stratiform profiles is obvious in the precipitation systems sampled in Brazil and in Florida (Table 4). The standard deviation of V_r above the freezing level in convective regions is 4–5 m s^{-1}, at least 2 times that for stratiform profiles. Frozen hydrometeors are carried up or down at 2 m s^{-1} or more at some level in almost all convective profiles, but in only about one-half of the stratiform profiles. Some 10% of the convective profiles even see hydrometeors below the freezing level carried upward, and rapid lifting (at over 4 m s^{-1}) is about one-half as frequent (Table 4). Yet, lofting below 4 km and rapid lifting virtually does not occur in stratiform regions. Florida convection tends to stand out as more vigorous than the convective profiles in Brazil. It is remarkable that in about one-half of the stratiform profiles in Florida, and nearly as many in Brazil, frozen hydrometeors are carried up or move down at 2 m s^{-1} or more. The downward motion of course is most common, but the fall speed of unrimed snow is less than 2 m s^{-1}. One factor to consider is that the vertical air motion is an instantaneous measure, but the fall speed is based on a history of particle growth. Imagine rimed snow falling down in a decaying isolated thunderstorm, with weak vertical motions. These hydrometeors fall at over 2 m s^{-1} yet still produce a BB or a large DVG (Zrnic et al. 1993).

The difference between the hurricane precipitation profiles and those elsewhere is highlighted again in Table 4. The variability of V_r values above the freezing level is relatively small in hurricanes, especially in the stratiform regions; it is less than one-half that of corresponding regions in Florida. Strong hydrometeor fountains may occur in the hurricane sample, but almost exclusively in the convective regions and less commonly than is observed in Florida and Brazil.

It should be mentioned that these statistics are affected by the uncertainty in V_r (section 2c). Both the standard deviation and the occurrence of extreme values are impacted. For instance, the $<1\%$ probability of rapid or shallow lifting in stratiform regions (last two columns in Table 4) is probably noise. Assuming a normal distribution of the errors, with a zero bias and a standard deviation of 1 m s^{-1}, then $|V_r| > 2$ m s^{-1} can still be expected in 4.6% of the cases, if in reality the hydrometeor vertical velocity is zero (the updraft balances the fall speed). This figure is small in comparison with the values in Table 4. It is remarkable also that the standard deviation of V_r is smallest in the hurricane sample, yet the mean bias of the unadjusted V_r at the earth's surface and the error induced by horizontal winds contributing to the radial velocity in a slightly off-nadir beam are largest there (section 2c). Clearly the standard deviation of V_r is dominated by true atmospheric processes, not measurement uncertainty. Thus, the general patterns revealed in Table 4 are valid.

4. Discussion

The classification method presented herein (Fig. 2) is fundamentally different from texture methods. Our method, based on the one by Williams et al. (1995) developed for 915-MHz wind profiler data, uses the vertical reflectivity and Doppler velocity profiles to single out stratiform precipitation. Texture methods use the horizontal reflectivity field to single out convective regions (e.g., Churchill and Houze 1984; Steiner et al. 1995). Even though our method classifies profiles individually, without proximity criteria, they appear consistent with the texture methods, in the sense that they identify stratiform and convective regions that are continuous over some distance along the flight track, and that are of a realistic width. Also, the vertical motion characteristics are physically consistent with the rain-type identity: more variability is found in the particle vertical motion in convective regions compared to stratiform regions, and fountains of hydrometeors (Houze 1997, Fig. 1) are clearly present in convective regions.

The analysis of the classification results, the melting-layer signature of stratiform profiles, and the hydrometeor vertical velocity characteristics is focused on three different regions. This analysis showed that in hurricanes stratiform precipitation is dominant, that stratiform regions are larger, that stratiform profiles are more clearly defined, and that the variability of hydrometeor vertical motion is relatively small. All of this points to the fundamentally different nature of tropical cyclone precipitation, compared to that in isolated or organized tropical convection. These differences will be examined further in Part II, which aims to use the classification of tropical precipitation profiles to characterize reflectivity and velocity profiles and coincident passive microwave signatures in Florida, Brazil, and hurricanes.

5. Summary

Airborne measurements of vertical incidence radar reflectivity and Doppler velocity are analyzed to classify and describe tropical precipitation systems. The classification can be used by vertical incidence radars only, which do not sample the two-dimensional horizontal echo structure. The key classification argument is the presence of a melting-layer signature that characterizes stratiform precipitation, including a bright band (BB) and a large vertical Doppler velocity gradient (DVG). The detection of this signature is used as the basis of the classification of rain profiles as stratiform, convective, or warm. This detection is unambiguous in the case of the ER-2 Doppler radar (EDOP), given EDOP's high vertical resolution (37.5 m) and sensitivity. The classification method identifies stratiform and convective

regions of a realistic size. The vertical motion characteristics are physically consistent with rain-type identity: hydrometeors are carried up and down by small-scale drafts in convective regions, resulting in a variance of the hydrometeor vertical motion that is about 2 times that in stratiform regions.

Some 21 231 km of flight tracks over tropical precipitation systems are analyzed. This includes convective systems of various sizes in central Florida and in southwestern Amazon, and several hurricanes. The sample size is too small for a climatology of precipitation systems, but it is large enough to note some outstanding characteristics.

Hurricanes are more stratiform, and their stratiform nature is defined better than storms in southwestern Amazon and especially in central Florida. The better definition is evidenced by the good agreement between the BB and DVG aspects of the melting-layer signature, and the detectability of the BB even under degraded vertical resolutions. Both convective and stratiform regions in land-based storms are quite diverse in terms of the vertical structure of reflectivity and Doppler velocity. The composite vertical structure of the various rain types in hurricanes, as well as in isolated to organized convection sampled in Florida and Brazil, will be explored in Part II.

Acknowledgments. This work was supported by NASA EPSCoR Grant 5-33395. We appreciate the assistance of Q. Miao with data processing and Dr. G. Heymsfield in the preparation and the analysis of the data. This work also benefited from the input from Dr. R. Houze and several other critical reviews.

APPENDIX

Hydrometeor Fall Speed Estimation

The vertical air motion w is the difference between the nadir beam radial velocity V_r (corrected for aircraft motion), which represents the hydrometeor vertical motion, and the terminal velocity of the hydrometeors V_p:

$$w = -V_r - (-V_p).$$

Here, both V_r and V_p are positive downward. This explains the minus signs. For hurricanes we use the $Z - V_p$ relations given in Marks and Houze (1987):

$$V_{pr} = 2.6Z^{0.107} \quad \text{and} \quad V_{ps} = 0.817Z^{0.063}.$$

Marks and Houze use the rain equation (V_{pr}) below 5.1 km and the snow equation (V_{ps}) above 7.5 km. Even in the eyewall of hurricanes, the freezing level is found to be lower than 5.1 km; therefore, in this study the fall speed is linearly interpolated between that of snow and that of rain between 3.5 and 5 km. The fall speed equations listed above apply to sea level. For a correction of air density, Foote and DuToit (1969) suggest $V_{ps} = V_{pso}(\rho_o/\rho)^{0.4}$, or approximately $V_{ps} = V_{pso} \exp(h/21.3)$, where h is the height (km), and V_{pso} is the fall speed V_{ps} at sea level where the air density ρ is ρ_o.

In other precipitation systems, the terminal velocity of raindrops can be estimated as $V_{pr} = aD^b$, where $a = 3.86$, and $b = 0.67$ [Doviak and Zrnic 1992, their Eq. (8.4)], where V_{pr} is expressed in meters per second and D is in millimeters. It is further assumed that the hydrometeor sizes follow a Marshall–Palmer distribution,

$$N_D = N_0 e^{-\Lambda D},$$

where $N_0 = 8000\ \text{m}^{-3}\ \text{mm}^{-1}$ for rain. In that case the mean reflectivity-weighted terminal velocity of rain can be related to radar reflectivity Z as follows:

$$\overline{V}_{pr} = \frac{a\Gamma(7 + b)}{\Lambda^b \Gamma(7)},$$

where

$$\Lambda = \left[\frac{N_0\Gamma(7)}{Z}\right]^{1/7}.$$

Above the radar bright band, hydrometeors are assumed to be mostly snow with a terminal velocity of $V_{ps} = aD^b$,where $a = 0.98$, and $b = 0.31$ [Doviak and Zrnic 1992, their Eq. (8.6d)], where V_{ps} (m s^{-1}) is the fall speed of snow and D (mm) is the equivalent diameter of a snowflake. For snow, a Marshall–Palmer distribution is assumed as well, with the same value for N_0, with

$$\Lambda = \left[\frac{N_0\Gamma(7)|K_i|^2}{Z|K_w|^2}\right]^{1/7},$$

where $|K_i|^2 = 0.197$ and $|K_w|^2 = 0.93$ are the dielectric factors for ice particles and water droplets, respectively (Battan 1973). The differences between the resulting Z–V_p relationships, and those in Marks and Houze (1987) are less than 1 m s^{-1} for rain and less than 0.2 m s^{-1} for snow, for all reflectivity values. The Marks and Houze (1987) V_p estimates are generally lower.

In the presence of graupel, a terminal velocity of $V_{pg} = aD^b$, where $a = 1.30$, and $b = 0.66$ [Doviak and Zrnic 1992, their Eq. (8.6c)] is assumed. If the reflectivity exceeds 45 dBZ above the freezing level, the hydrometeors are assumed to be graupel. If it is less than 35 dBZ, the fall speed of snow is used. Where the reflectivity falls between 35 and 45 dBZ, the fall speed of hydrometeors is a linear combination of V_{ps} and V_{pg}. The corrections for altitude and the assumed transition between the fall speeds of rain and snow within the brightband zone are the same as for hurricanes.

REFERENCES

Atlas, D., 1966: The balance level in convective storms. *J. Atmos. Sci.*, **23,** 635–651.

Battan, L. J., 1973: *Radar Observation of the Atmosphere.* University of Chicago Press, 324 pp.

Biggerstaff, M. I., and S. A. Listemaa, 2000: An improved scheme for convective/stratiform echo classification using radar reflectivity. *J. Appl. Meteor.,* **39,** 2129–2150.

Churchill, D. D., and R. A. Houze Jr., 1984: Development and structure of winter monsoon cloud clusters on 10 December 1978. *J. Atmos. Sci.,* **41,** 933–960.

Donaldson, R. J., 1961: Radar reflectivity profiles in thunderstorms. *J. Atmos. Sci.,* **18,** 292–305.

Doviak, R. J., and D. S. Zrnic, 1992: *Doppler Radar and Weather Observations.* 2d ed. Academic Press, 562 pp.

Emanuel, K. A., 1986: An air–sea interaction theory for tropical cyclones. Part I: Steady-state maintenance. *J. Atmos. Sci.,* **43,** 585–604.

Foote, G. B., and P. S. Du Toit, 1969: Terminal velocity of raindrops aloft. *J. Appl. Meteor.,* **8,** 249–253.

Gage, K. S., C. R. Williams, W. L. Clark, P. E. Johnston, and D. A. Carter, 2002: Profiler contributions to Tropical Rainfall Measuring Mission (TRMM) ground validation field campaigns. *J. Atmos. Oceanic Technol.,* **19,** 843–863.

Geerts, B., and Y. Dawei, 2004: Classification and characterization of tropical precipitation based on high-resolution airborne vertical incidence radar. Part II: Composite vertical structure of hurricanes versus storms over Florida and the Amazon. *J. Appl. Meteor.,* **43,** 1567–1585.

——, G. M. Heymsfield, L. Tian, J. B. Halverson, A. Guillory, and M. I. Mejia, 2000: Hurricane Georges' landfall in the Dominican Republic: Detailed airborne Doppler radar imagery. *Bull. Amer. Meteor. Soc.,* **81,** 999–1018.

Goldhirsh, J., and B. Musiani, 1986: Rain cell size characteristics derived from radar observations at Wallops Island, Virginia. *IEEE Trans.Geosci. Remote Sens.,* **GE-24,** 947–954.

Heymsfield, G. M., 1989: Accuracy of vertical air motions from nadir-viewing Doppler airborne radars. *J. Atmos. Oceanic Technol.,* **6,** 1079–1082.

——, and L. Tian, 2000: Fallspeeds and vertical air motions in stratiform rain derived from ER-2 Doppler radar observations. Preprints, *13th Int. Conf. on Clouds and Precipitation,* Reno, NV, International Union of Geodesy and Geophysics, 303–305.

——, and Coauthors, 1996: The EDOP radar system on the high-altitude NASA ER-2 aircraft. *J. Atmos. Oceanic Technol.,* **13,** 795–809.

——, B. Geerts, and L. Tian, 2000: TRMM precipitation radar reflectivity profiles as compared with high-resolution airborne and ground-based radar measurements. *J. Appl. Meteor.,* **39,** 2080–2102.

——, J. B. Halverson, J. Simpson, L. Tian, and T. P. Bui, 2001: ER-2 Doppler radar investigations of the eyewall of Hurricane Bonnie during the Convection and Moisture Experiment-3. *J. Appl. Meteor.,* **40,** 1310–1330.

Hobbs, P. V., N. T. Funk, R. R. Weiss, J. D. Locatelli, and K. R. Biswas, 1985: Evaluation of a 35 GHz radar for cloud physics research. *J. Atmos. Oceanic Technol.,* **2,** 35–48.

Houze, R. A., Jr., 1973: A climatological study of vertical transports by cumulus-scale convection. *J. Atmos. Sci.,* **30,** 1112–1123.

——, 1993: *Cloud Dynamics.* Academic Press, 573 pp.

——, 1997: Stratiform precipitation in regions of convection: A meteorological paradox? *Bull. Amer. Meteor. Soc.,* **78,** 2179–2196.

——, F. D. Marks, and R. A. Black, 1992: Dual-aircraft investigation of the inner core of Hurricane Norbert. Part II: Mesoscale distribution of ice particles. *J. Atmos. Sci.,* **49,** 943–963.

Iguchi, T., T. Kozu, R. Meneghini, J. Awaka, and K. Okamoto, 2000: Rain-profiling algorithm for the TRMM precipitation radar. *J. Appl. Meteor.,* **39,** 2038–2052.

Johnson, R. H., T. M. Rickenbach, S. A. Rutledge, P. E. Ciesielski, and W. H. Schubert, 1999: Trimodal characteristics of tropical convection. *J. Climate,* **12,** 2397–2418.

Lee, W.-C., P. Dodge, F. D. Marks, and P. H. Hildebrand, 1994: Mapping of airborne Doppler radar data. *J. Atmos. Oceanic Technol.,* **11,** 572–578.

López, R. E., 1976: Radar characteristics of the cloud populations of tropical disturbances in the northwest Atlantic. *Mon. Wea. Rev.,* **104,** 268–283.

Marks, F. D., Jr., and R. A. Houze Jr., 1987: Inner core structure of Hurricane Alicia from airborne Doppler radar observations. *J. Atmos. Sci.,* **44,** 1296–1317.

——, ——, and J. F. Gamache, 1992: Dual-aircraft investigation of the inner core of Hurricane Norbert. Part I: Kinematic structure. *J. Atmos. Sci.,* **49,** 919–942.

NASDA, 1999: TRMM PR algorithm instruction manual V1. 0. Communications Research Laboratory, 52 pp. [Available from Communications Research Laboratory, 4-2-1 Nukui-kitamachi, Koganei-chi, Tokyo 184, Japan.]

Petersen, W. A., and S. A. Rutledge, 2001: Regional variability in tropical convection: Observations from TRMM. *J. Climate,* **14,** 3566–3586.

——, S. W. Nesbitt, R. J. Blakeslee, R. Cifelli, P. Hein, and S. A. Rutledge, 2002: TRMM observations of intraseasonal variability in convective regimes over the Amazon. *J. Climate,* **15,** 1278–1294.

Rosenfeld, D., E. Amitai, and D. B. Wolff, 1995: Classification of rain regimes by the three-dimensional properties of reflectivity fields. *J. Appl. Meteor.,* **34,** 198–211.

Sauvageot, H., F. Mesnard, and R. S. Tenorio, 1999: The relation between the area-average rain rate and the rain cell size distribution parameters. *J. Atmos. Sci.,* **56,** 57–70.

Schumacher, C., and R. A. Houze Jr., 2003: Stratiform rain in the Tropics as seen by the TRMM precipitation radar. *J. Climate,* **16,** 1739–1756.

Steiner, M., and R. A. Houze Jr., 1997: Sensitivity of the estimated monthly convective rain fraction to the choice of *Z–R* relation. *J. Appl. Meteor.,* **36,** 452–462.

——, ——, and S. E. Yuter, 1995: Climatological characterization of three-dimensional storm structure from operational radar and raingauge data. *J. Appl. Meteor.,* **34,** 1978–2007.

Stewart, R. E., J. D. Marwitz, J. C. Pace, and R. E. Carbone, 1984: Characteristics through the melting layer of stratiform clouds. *J. Atmos. Sci.,* **41,** 3227–3237.

Testud, J., P. H. Hildebrand, and W.-C., Lee, 1995: A procedure to correct airborne Doppler radar data for navigation errors using the echo returned from the earth's surface. *J. Atmos. Oceanic Technol.,* **12,** 800–820.

Tian, L., G. M. Heymsfield, and R. C. Srivastava, 2002: Measurement of attenuation with airborne and ground-based radar in convective storms over land and its microphysical implications. *J. Appl. Meteor.,* **41,** 716–733.

Tokay, A., D. A. Short, C. R. Williams, W. L. Ecklund, and K. L. Gage, 1999: Tropical rainfall associated with convective and stratiform clouds: Intercomparison of disdrometer and profiler measurements. *J. Appl. Meteor.,* **38,** 302–320.

White, A. B., D. J. Gottas, E. T. Strem, F. M. Ralph, and P. J. Neiman, 2002: An automated brightband height detection algorithm for use with Doppler radar spectral moments. *J. Atmos. Oceanic Technol.,* **19,** 687–697.

Williams, C. R., W. L. Ecklund, and K. S. Gage, 1995: Classification of precipitating clouds in the Tropics using 915-MHz wind profilers. *J. Atmos. Oceanic Technol.,* **12,** 996–1012.

Zrnic, D. S., N. Balakrishnan, C. L. Ziegler, V. N. Bringi, K. Aydin, and T. Matejka, 1993: Polarimetric signatures in the stratiform region of a mesoscale convective system. *J. Appl. Meteor.,* **32,** 678–693.